iScience, Volume *23*

Supplemental Information

Lymph Node Subcapsular Sinus Microenvironment-On-A-Chip Modeling Shear Flow Relevant to Lymphatic Metastasis and Immune Cell Homing

Katherine G. Birmingham, Meghan J. O'Melia, Samantha Bordy, David Reyes Aguilar, Bassel El-Reyas, Gregory Lesinski, and Susan N. Thomas

Transparent Methods

Cell Culture

THP-1 monocytes were cultured RPMI-1640 supplemented with 10% heat inactivated fetal bovine serum and 1% penicillin/streptomycin/amphotericin B. PANC-1 cells were cultured in Dulbecco's Modified Eagle Medium supplemented with 10% heat inactivated fetal bovine serum, 1% penicillin/streptomycin/amphotericin B, and 1% Glutamax. Parental and Phamret-expressing (Edwards et al., 2018) human colorectal adenocarcinoma LS174T cells were cultured in Dulbecco's Modified Eagle Medium supplemented with 10% heat inactivated fetal bovine serum and 1% penicillin/streptomycin/amphotericin B. For perfusion experiments, LS174T and PANC-1 cells were harvested via mild trypsinization with 0.25% trypsin/ethylenediaminetetraacetic acid, centrifuged at 400 X G for 5 min, resuspended in culture medium, and incubated in suspension for 2 h at 37°C to allow regeneration of adhesive cell surface ligands prior to centrifugation and resuspension in perfusion medium [0.1 % bovine serum albumin (BSA) in D-PBS with calcium and magnesium] and subsequent storage on ice until use (< 1 h). THP-1 cells were directly harvested (without trypsinization), centrifuged at 400 X G for 5 min, and resuspended in perfusion medium for storage on ice until use (< 1 h). B16F10 cells were cultured in Dulbecco's Modified Eagle Medium with 10% heat-inactivated fetal bovine serum and 1% penicillin/streptomycin/amphotericin B and harvested by trypsinization prior to use *in vivo* experimentation.

LN immunohistochemistry, imaging, and analysis

Brachial LNs from naïve C57Bl6 mice or draining melanomas 7 d post intradermal implantation in the lateral dorsal skin with $5x10^5$ B16F10 cells (Rohner et al., 2015) were surgically excised, embedded in optimum cutting temperature embedding medium, and stored at -80°C. A cryostat was used to slice 10 µm thick tissue sections that were mounted onto histological slides and stored at -20°C. Sections were acetone fixed for 20 min at -20°C, blocked with 10% goat serum diluted in Dulbecco's Phosphate Buffered Saline (D-PBS) with calcium and magnesium for 1 h at room temperature, and incubated overnight at 4°C with the following primary antibodies: (1) rabbit anti-mouse LYVE-1 (1:200, Invitrogen, PA1-16635), (2) chicken anti-mouse CD62E (1:100, Novus Biologicals, AF575), and (3) hamster anti-mouse CD54 (1:100, Novus Biologicals, NBP2-22540) or rat anti-mouse CD106 (1:50, Novus Biologicals, NB100-77474). The following day, the slides were incubated for 1 h at room temperature with the following fluorophore conjugated secondary antibodies: (1) goat anti-rabbit Alexa Flour 633 (1:300, Invitrogen, A-21070), (2) goat anti-chicken Alexa Flour 488 (1:200, Invitrogen, A-11039), and (3) goat anti-hamster DyLight 550 (1:1000, Novus Biologicals, NBP1-71730R) or goat anti-rat DyLight 550 (1:100, Invitrogen, SA5-10019). In between each staining step, slides were washed three times with gentle agitation in 0.1% Tween 20 diluted in D-PBS with calcium and magnesium. Washed slides were mounted using Vectashield mounting medium with DAPI and microscopic images were taken using a Zeiss 710 confocal microscope. Collagen structures of whole LNs pre-treated with increasing concentrations of 2-2' thiodiethanol (10, 25, 50, 97%) for 10-30 min prior to mounting in Fluorogel were imaged in 2 µm intervals up to a 100 µm tissue depth using two-photon microcroscopy collecting

the collagen second harmonic on a LSM 510 confocal microscope up to 100 um depth. SCS heights were measured using Zen Black Software.

COMSOL Modelling

WSS profiles along the SCS floors were modeled using COMSOL Multiphysics Software version 5.4. An idealized LN sinus was designed in SolidWorks, modeling the afferent lymphatic vessel as a cylinder leading fluid to radially disperse into the LN SCS modeled as a thin disk (Figure 2B). Various LN dimensions, including the afferent LVD and SCS height were used to construct three variations of the idealized LN luminal geometry (Figure 2B), while the upper limit of the SCS radius was maintained at 5 mm and 0.5 mm was chosen based on the average size of human and mouse LNs, respectively (Jafarnejad et al., 2015; Kikuchi et al., 2020; Takeda et al., 2017). LN geometries were exported as .STL files and imported into COMSOL. Within COMSOL, the fluid material was defined as a Newtonian, incompressible fluid with a dynamic viscosity of 1800 Pa s and density of 1009 kg m^{-3} (Moore and Bertram, 2018). The fluid flow was set to laminar flow with a constant volumetric flow rate of 1.33E-10 $m^3 s^{-1}$, which is within the range of flow rates observed in humans (Blatter et al., 2016). The boundary walls were chosen to be the outer surface of the liquid domain, the inlet was defined as the top of the afferent vessel cylinder, and the outlet was defined to be the circumferential side wall of the SCS thin disc. The boundaries were set as impermeable. Finally, the cut plane where the WSS values were quantified was defined as the bottom of the thin disc (z = 0, Figure 2I), representing the inferior floor of the LN SCS.

The Particle Tracing for Fluid Flow module of COMSOL Multiphysics Software version 5.4 was used to simulate cell trajectories during movement from the afferent vessel into the LN SCS and to determine the location at which cells were in close proximity with the inferior surface of the SCS. Particle properties were modeled after that of cancerous cells, with a diameter of 14 μm and a mass density of 1032 kg m^{-3} (Moore and Bertram, 2018). The same inlet, outlet, flow rate, fluid properties, and boundary walls as used in the WSS modeling described were used in particle trajectory simulations. For each simulation, a particle (cell) began its flow trajectory through the geometry at the top of the afferent vessel (2.5 mm from the SCS floor) in a randomly selected radial position (less than or equal to one half the diameter of the afferent vessel), and the height and radial position of the particle was tracked until it reached the periphery of the SCS. The particle was defined as settled on the SCS floor when the center of the particle was at a height of 7 μm, the particle radius.

Channel Fabrication

Microfluidic channels were fabricated in a manner similar to that detailed previously (Birmingham et al., 2019b; Erin Elizabeth Edwards et al., 2018; Tran et al., 2017). Briefly, the adhesive microfluidic channel, which consisted of a straight 10 cm long by 0.2 cm wide section connected to a 4 cm long divergent section that increased in width from 0.2 cm to 1.2 cm, was cut from sheet of 125 μm thick double-sided adhesive tape backed with a release liner. The channel was then affixed to polydimethylsiloxane, which was previously cured by mixing polydimethylsiloxane base with curing agent at a ratio of 9:1 and curing at 90˚C for 3 h in a Pyrex dish prior to being cut to the outer dimensions of the

channel shape. An inlet hole was punched into the beginning of the long, straight portion of the channel using a 3 mm biopsy punch, and the construct was attached to a non-tissue culture treated polystyrene plates into which an outlet hole was drilled prior to assembly.

Channel Functionalization

The short, divergent portion of the channel nearest the outlet was functionalized by incubation overnight at 4°C with Fc specific anti-IgG diluted in D-PBS without calcium and magnesium to a concentration of 2.5, 5, or 12.5 μg mL^{-1} for eventual use with E-selectin alone or in combination with 2.5 μg mL^{-1} ICAM or VCAM or 10 μg mL^{-1} VCAM experiments, respectfully. Next, plates were blocked for 1 h at room temperature with 1% BSA in D-PBS with calcium and magnesium after which E-selectin alone or in addition to either ICAM or VCAM diluted in D-PBS with calcium and magnesium was incubated for 2 h at room temperature. The entire channel was blocked for 1 h at room temperature with 1% BSA in D-PBS with calcium and magnesium at room temperature, after which plates were washed and immediately used in perfusion experiments. In between each step, the channel was washed three times with 1 mL of D-PBS with calcium and magnesium.

Perfusion Experiment Workflow

Perfusion experiments were performed in a similar manner to that formerly described (Birmingham et al., 2019b). Succinctly, an inlet syringe connected to tubing filled with perfusion media was connected to a syringe pump and used to withdraw a cell

pulse into the inlet tubing at a rate of 0.5 mL min^{-1}. For perfusion experiments using a single cell type, the cell pulse consisted of $2x10^5$ LS174T, PANC-1, or THP-1 cells diluted in 125 µL of perfusion media. The tubing and syringe assembly was inserted into the inlet hole of the channel and an outlet reservoir was made by connecting a 5 mL test tube to the bottom of the drilled outlet hole on the polystyrene plate. The assembled platform was placed on an Eclipse TI optical microscope with an objective magnification of 10X and linked to NIS-Elements software to acquire videos at a frame rate of 25 frames per sec at an exposure time of 0.281 µsec and 2x2 binning of a 500 by 376 pixels.

To begin perfusion, the syringe pump was set to a constant flow rate, based on desired WSS ranges of different LN flow models, to initiate inflow into the channel from the syringe-tubing assembly. Flow rates of 34.7, 27.4, and 9.7 mL min^{-1} were used to model quiescent LN, dilated LVD, and dilated SCS flows, respectively. Once cells reached the divergent portion of the channel during perfusion experiments, 30 sec videos were taken along the center line of the channel at 0.5 cm increments using the integrated Nikon camera. Perfusions were continued until all cells, except those that firmly adhered to the functionalized portion of the channel, eluted from the device as determined by the lack of any rolling cells within the functionalized portion as verified by videomicroscopy.

LS174T Cell and THP-1 Cell Coperfusion Workflow

For studies involving the co-perfusion of LS174T in combination with THP-1 cells, 125 µL total volume cell pulse was made by diluting 10^5 Phamret-expressing LS174T cells with 0, $0.33x10^5$, $1.0x10^5$, or $3.0x10^5$ THP-1 monocytes immediately before perfusion. Furthermore, the Phamret-expressing LS174T cells were pre-photoconverted

prior to perfusion to permit the visualization of the LS174T cells, but not the THP-1 cells, using a fluorescein isothiocyanate filter (Birmingham et al., 2020; Edwards et al., 2018). The perfusion workflow and adhesion quantification was the same as described above, save adhesion by fluorescent LS174T cells being imaged using a fluorescein isothiocyanate filter (excitation bandpass 475-492 nm, emission bandpass 505-535 nm) with a Chroma Technology 100W PhotoFluor mercury lamp with same microscope using an exposure time of 200 ms.

Quantification of Adhesive Cell Behavior

An adhering cell was defined as one that was seen to exhibit horizontal translation at a velocity substantially slower than the non-interacting cells, e.g. those transiting the imaging field of view at the calculated free fluid velocity as well as cell velocities observed when perfused over unfunctionalized channels. Individual cell velocities over 30 sec intervals were quantified using ImageJ with a manual particle tracking plugin.

Statistical Analysis

Statistical significance was defined as $p<0.05$ following one- or two-way ANOVA and post hoc analysis or linear regression using the analysis tools in Graphpad Prism 8.

Supplemental Figures

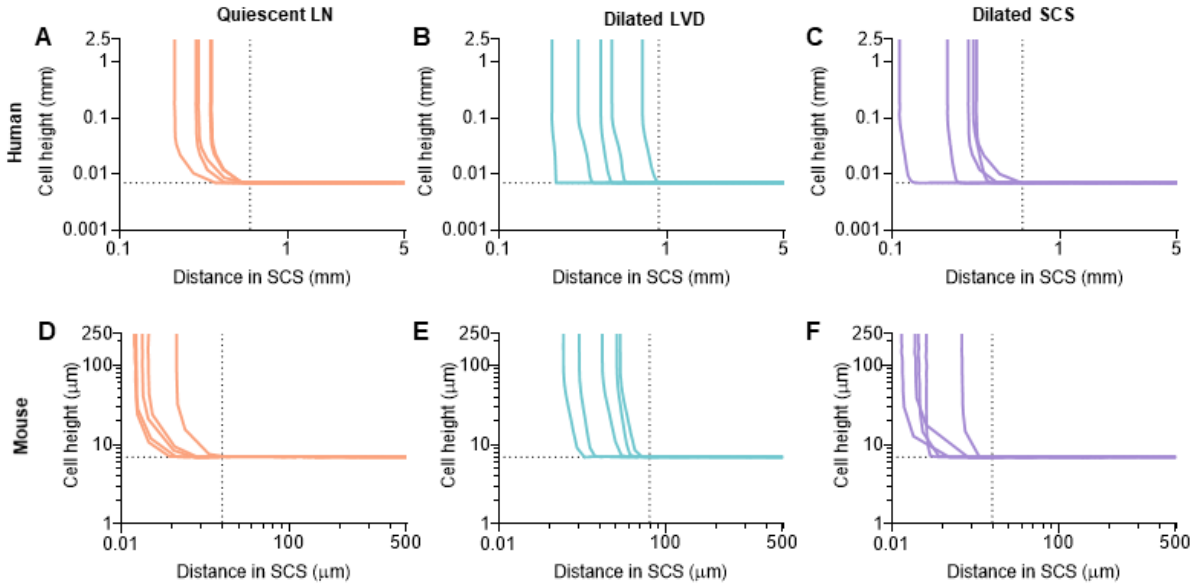

Figure S1. Computationally modelled trajectories of cells entering the LN SCS, related to Figures 2 and 3. COMSOL cell trajectory simulations using (A-C) human or (D-F) mouse LN parameters showing the position of the center of a cell of diameter 14 μm as it moves from the afferent lymphatic vessel into the SCS. Each colored line represents the trajectory of a single cell with a randomized radial starting location at the top of the afferent vessel. Dashed line on y-axis at a height of 7 μm, indicating the cell has settled to the bottom of the SCS floor. Dashed line on x-axis represent afferent vessel radius of (A,C) 0.6 mm (quiescent afferent LVD, human), (B) 0.9 mm (dilated LVD, human), (D,F) 40 μm (quiescent LVD, mouse), (E) 80 μm (dilated LVD, mouse).

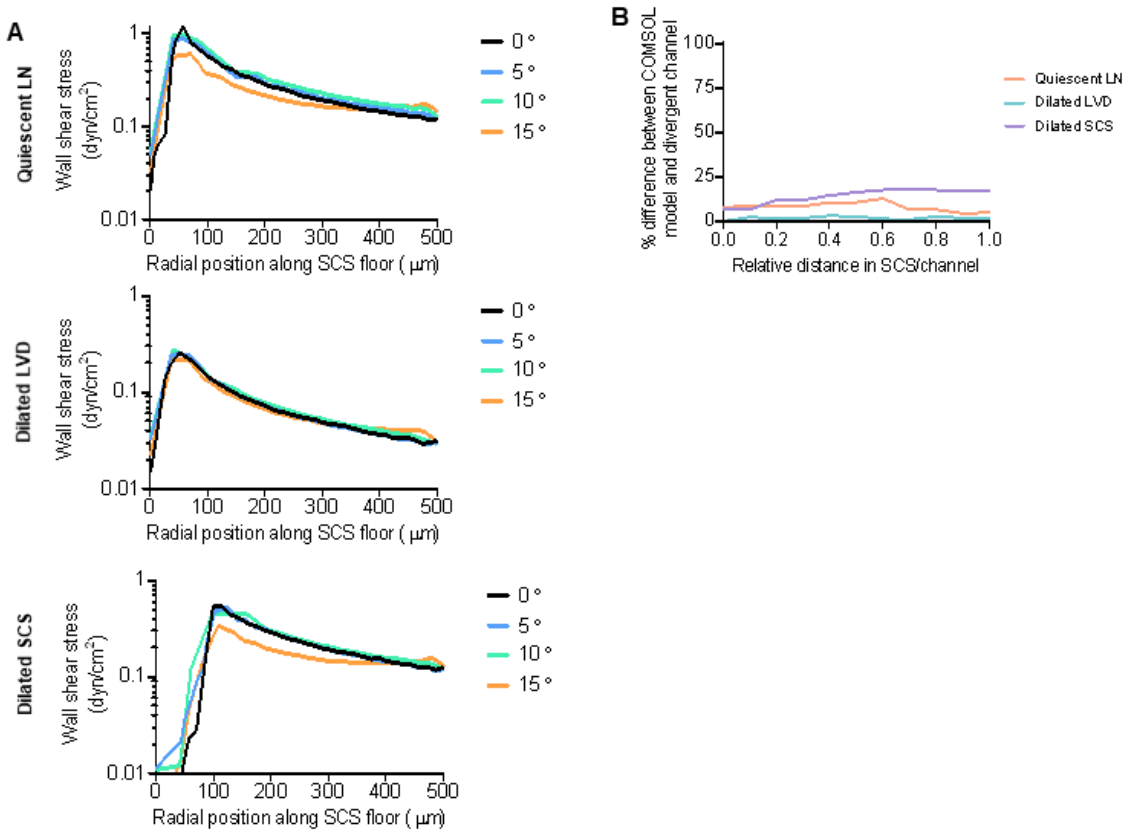

Figure S2. Computationally modelled effects of LN curvature effects on WSS and percent difference between COMSOL and divergent experimental flow model WSS profiles, related to Figures 2 and 3. (A) WSS levels predicted by COMSOL laminar fluid flow simulations through quiescent LNs (top), LNs with a dilated LVDs (middle), or LNs with a dilated SCS (bottom) with varying degrees of SCS curvature. (B) Percent difference between COMSOL and microfluidic experimental flow model WSS profiles.

Microfluidic model	Perfusion flow rate (µl/min)	WSS range (dyn/cm²)	Model LVD (µm)	Model SCS H (µm)
Quiescent LN	34.7	1 – 0.167	1.2	50
Dilated LVD	21.5	0.62 – 0.11	1.2	100
Dilated SCS	9.7	0.28 – 0.04	1.8	50

Table S1, related to Figure 3. Perfusion conditions used to model literature reported parameters human LNs.

Channel position (cm)	0	0.5	1	1.5	2	2.5	3	3.5	4
Microfluidic model	Wall Shear Stress (dyn/cm²)								
Quiescent LN	1.000	0.545	0.437	0.305	0.278	0.212	0.205	0.184	0.167
Dilated LVD	0.620	0.338	0.244	0.189	0.157	0.132	0.115	0.112	0.110
Dilated SCS	0.280	0.153	0.110	0.085	0.071	0.060	0.052	0.046	0.040

Table S2, related to Figure 3. WSS levels along the length of the divergent channel at different flow rates based on COMSOL simulations of human LN parameters.

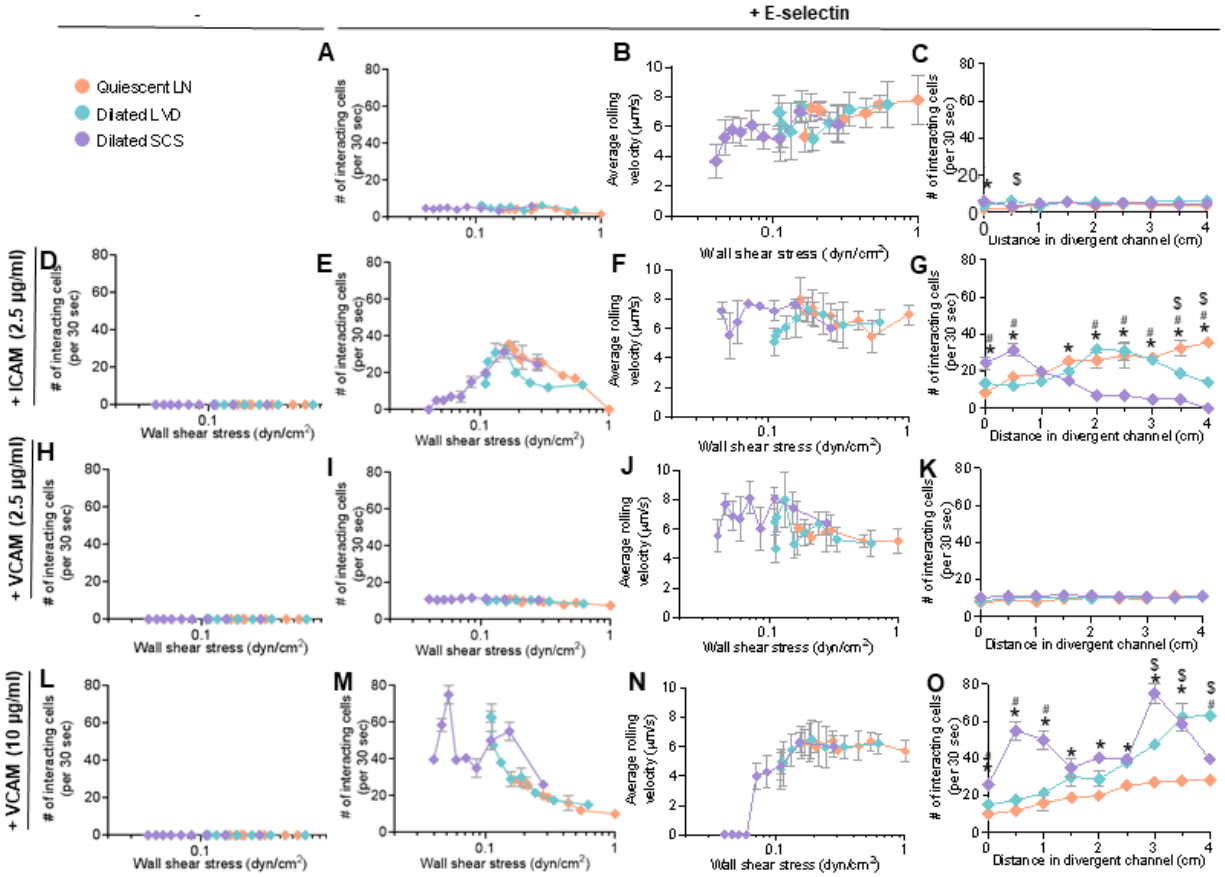

Figure S3. The WSS dependency of PANC-1 colon carcinoma cell adhesion in LN SCS-mimicking flow fields and microenvironments is altered by altered flow profiles predicted to result from LVD and SCS dilation, related to Figures 6 and 7. The number and average rolling velocity of PANC-1 cells adhering in flow in divergent channels functionalized with (A-C) 2.5 µg/mL E-selectin alone, (D) 2.5 µg/mL ICAM alone, (E-G) 2.5 µg/mL E-selectin + 2.5 µg/mL ICAM, (H) 2.5 µg/mL VCAM alone, (I-K) 2.5 µg/mL E-selectin + 2.5 µg/mL VCAM, (L) 10 µg/mL VCAM, or (M-O) 2.5 µg/mL E-selectin + 10 µg/mL VCAM. Statistical analysis by two-way ANOVA with post-hoc analysis between points at each channel position. $p < 0.05$ between: $ quiescent LN and dilated LVD, * quiescent LN and dilated SCS, and # dilated LVD and dilated SCS.

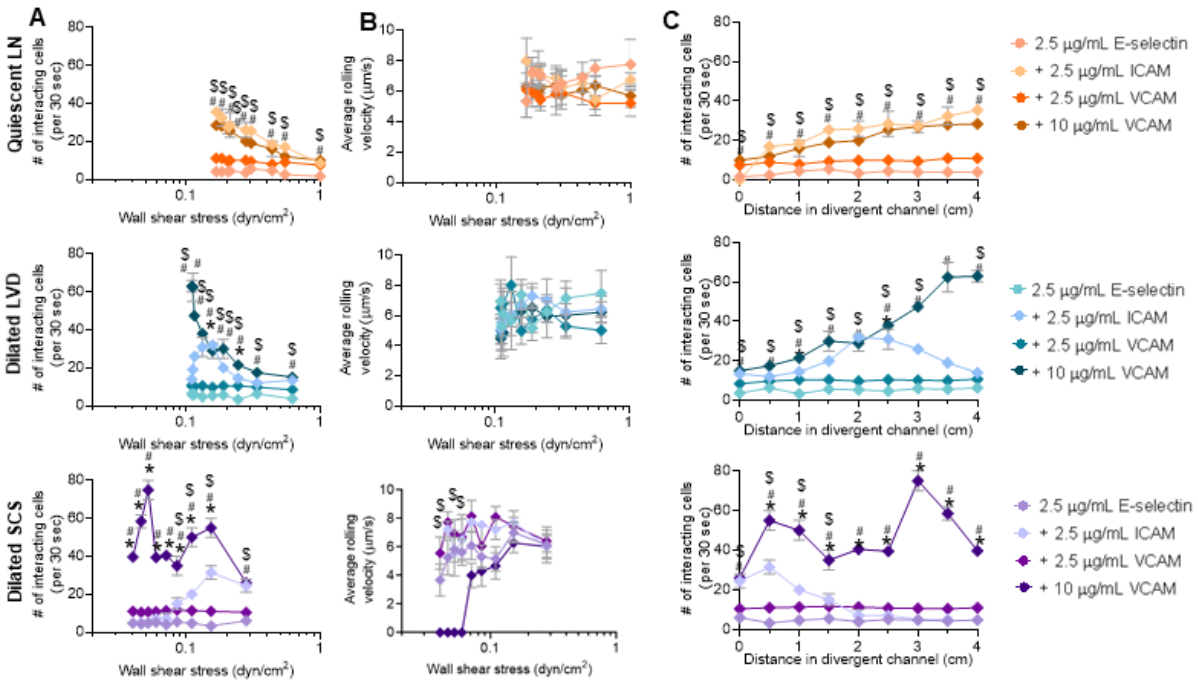

Figure S4. Co-presentation of adhesion molecules alters the WSS dependency of PANC-1 cell adhesion in flow, related to Figures 6 and 7. The number (A,C) and average rolling velocity (B) of PANC-1 cells adhering to E-selectin alone or when co-presented with ICAM or VCAM in flow regimes modelled after a quiescent LN (top row), LN with a dilated LVD (middle row), or LN with a dilated SCS (bottom row). Statistical analysis by unpaired t-test between points at each WSS or channel position. $p < 0.05$ between: $ E-selectin vs. E-selectin + 2.5 μg/mL ICAM, * E-selectin vs. E-selectin + 2.5 μg/mL VCAM, and # E-selectin vs. E-selectin + 10 μg/mL VCAM.

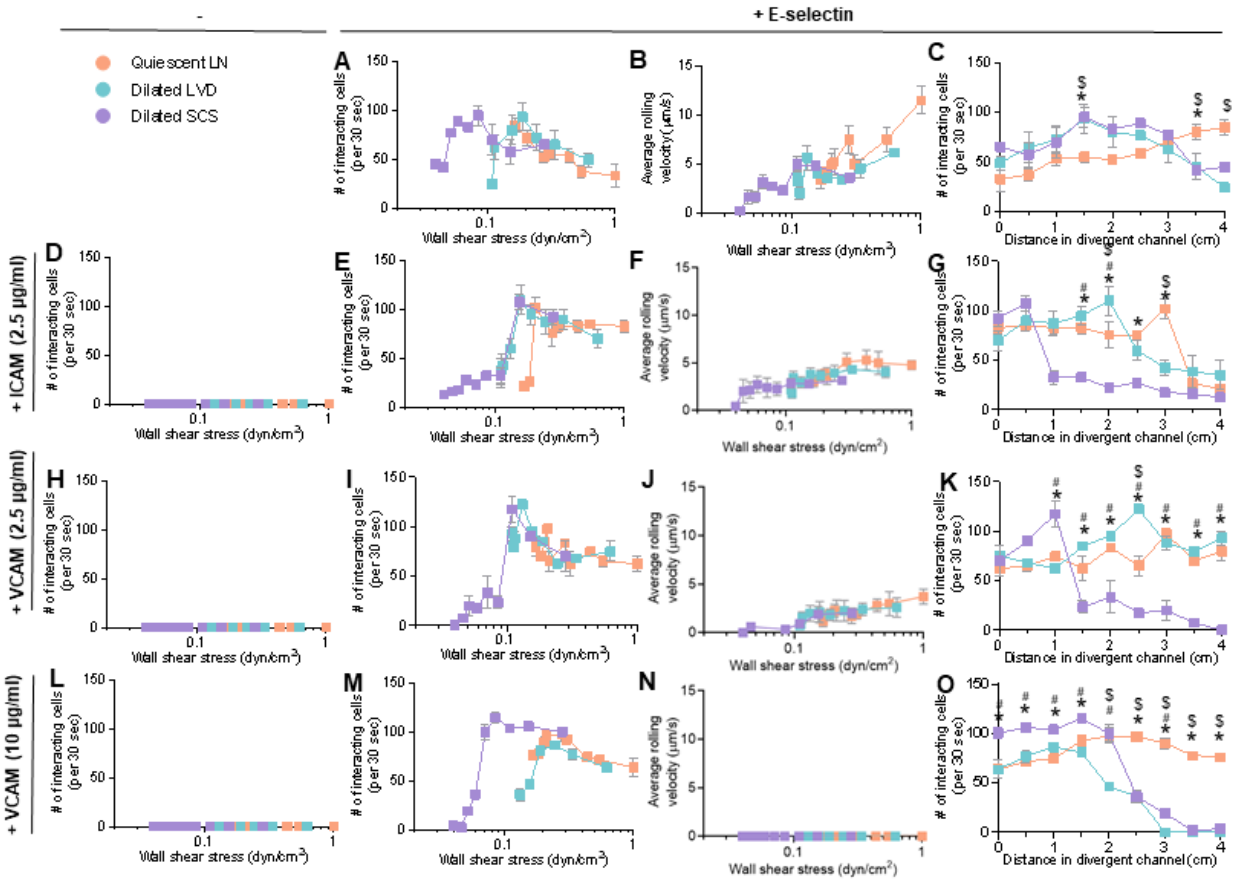

Figure S5. The WSS dependency of THP-1 colon carcinoma cell adhesion in LN SCS-mimicking flow fields and microenvironments is altered by altered flow profiles predicted to result from LVD and SCS dilation, related to Figures 6 and 7. The number and average rolling velocity of THP-1 cells adhering in flow in divergent channels functionalized with (A-C) 2.5 µg/mL E-selectin alone, (D) 2.5 µg/mL ICAM alone, (E-G) 2.5 µg/mL E-selectin + 2.5 µg/mL ICAM, (H) 2.5 µg/mL VCAM alone, (I-K) 2.5 µg/mL E-selectin + 2.5 µg/mL VCAM, (L) 10 µg/mL VCAM, or (M-O) 2.5 µg/mL E-selectin + 10 µg/mL VCAM. Statistical analysis by two-way ANOVA with post-hoc analysis between points at each channel position. $p < 0.05$ between: $ quiescent LN and dilated LVD, * quiescent LN and dilated SCS, and # dilated LVD and dilated SCS.

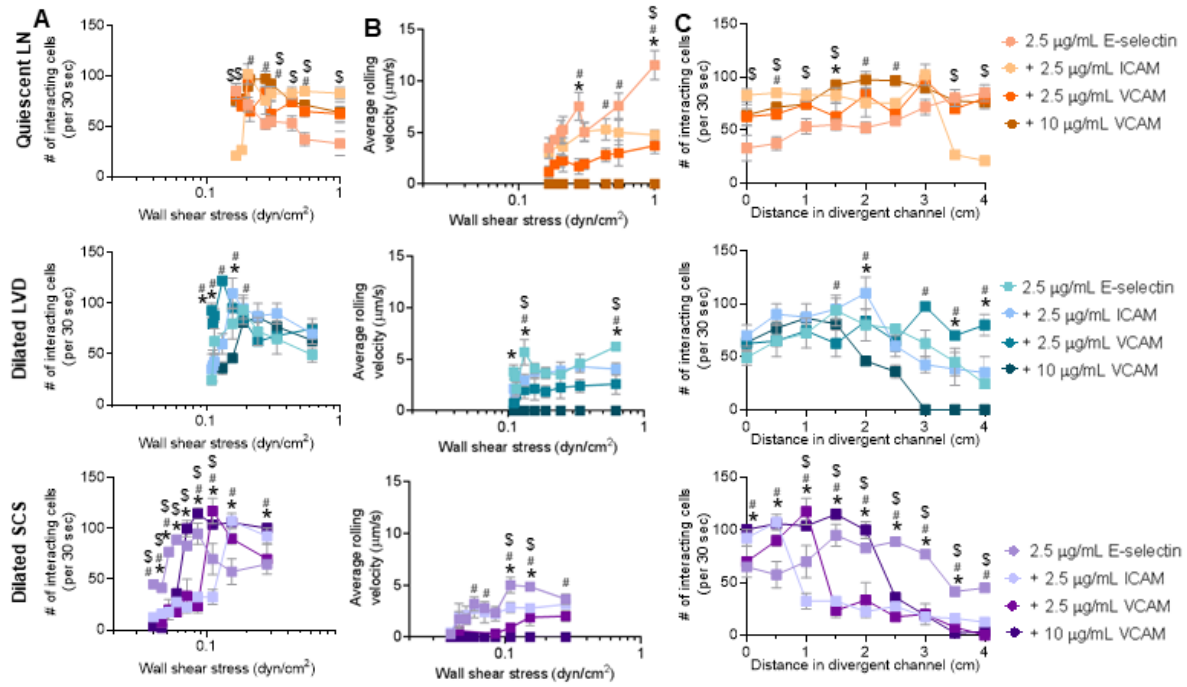

Figure S6. Adhesion molecule co-presentation alters WSS dependency of THP-1 adhesion in flow, related to Figures 6 and 7. The number (A,C) and average rolling velocity (B) of THP-1 cells adhering to E-selectin alone or when co-presented with ICAM or VCAM in flow regimes modelled after a quiescent LN (top row), LN with a dilated LVD (middle row), or LN with a dilated SCS (bottom row). Statistical analysis by two-way ANOVA with post-hoc analysis between points at each WSS or channel position. $p < 0.05$ between: $ E-selectin vs. E-selectin + 2.5 μg/mL ICAM, * E-selectin vs. E-selectin + 2.5 μg/mL VCAM, and # E-selectin vs. E-selectin + 10 μg/mL VCAM.

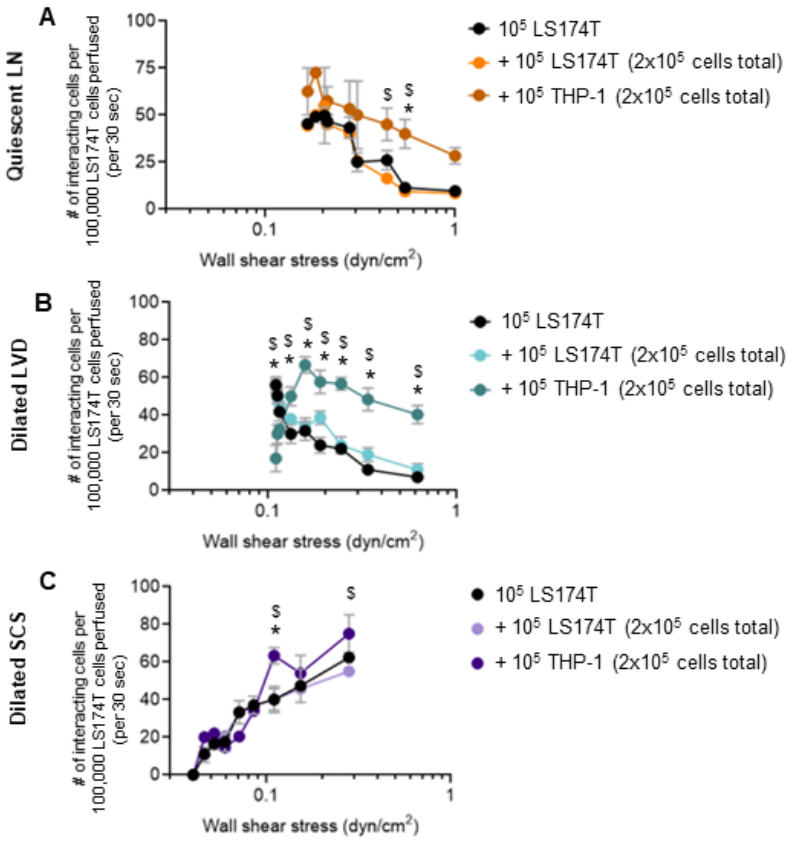

Figure S7. Increased adhesion by LS174T cells co-perfused with THP-1 cells is not due to steric interference, related to Figure 8. The number of LS174T cells mediating adhesion to E-selectin in flow when perfused alone (a total of 10^5 LS174T cells perfused) or during co-perfusion with either an additional 10^5 LS174T cells (total of $2x10^5$ LS174T cells perfused) or 10^5 THP-1 cells (total $2x10^5$ cells) in flows modeled after a (A) healthy LN, (B) LN with a dilated LVD, or (C) a LN with a dilated SCS. To adjust for differences in the number of perfused LS174T cell during a single cell perfusion of $2x10^5$ LS174T cells, the total number of interacting cells at each measured WSS was divided by two. Statistical analysis by two-way ANOVA with post-hoc analysis between points at each WSS. $p < 0.05$ between: \$ 10^5 LS174T vs + 10^5 LS174T, * 10^5 LS174T vs + 10^5 THP-1, and # + 10^5 LS174T vs. + 10^5 THP-1.